Journal of Nuclear Medicine, published on August 12, 2021 as doi:10.2967/jnumed.121.262430

Title: Imaging pituitary vasopressin 1B receptor in humans with the novel PET radiotracer ^{11}C-TASP699

Authors: Mika Naganawa[1], Nabeel B. Nabulsi[1], David Matuskey[1], Shannan Henry[1], Jim Ropchan[1], Shu-Fei Lin[1], Hong Gao[1], Richard Pracitto[1], David Labaree[1], Ming-Rong Zhang[2], Tetsuya Suhara[2], Izumi Nishino[3], Helene Sabia[4], Satoshi Ozaki[4], Yiyun Huang[1], Richard E. Carson[1]
[1]Yale PET Center, Department of Radiology and Biomedical Imaging, Yale University, New Haven, CT, USA
[2]National Institutes for Quantum and Radiological Science and Technology, Chiba, Japan
[3]Taisho Pharmaceutical Co., Ltd., Tokyo, Japan
[4]Taisho Pharmaceutical R&D Inc., Morristown, NJ, USA

Corresponding author:
Mika Naganawa, Ph.D.
PO Box 208048, New Haven, CT, 06520-8048, USA
Ph:203-737-5582, Fx:203-785-3107
mika.naganawa@yale.edu

Word Count:5000/5000

Running Title: Kinetic analysis of pituitary V_{1B} tracer

Acknowledgement: The clinical trial registration identifier of this study is NCT02448212. We appreciate the excellent technical assistance of the staff at the Yale University PET Center. We would like to thank Dr. Shigeyuki Chaki for reviewing this manuscript.

ABSTRACT

Arginine vasopressin (AVP) is a hormone that is mainly synthesized in the hypothalamus and stored in the posterior pituitary. Receptors for vasopressin are categorized into at least three subtypes (V_{1A}, V_{1B}, V_2). Among these subtypes, the V_{1B} receptor (V_{1B}R), highly expressed in the pituitary, is a primary regulator of the hypothalamic-pituitary-adrenal axis activity, and thus a potential target for the treatment of neuropsychiatric disorders, such as depression and anxiety. ^{11}C-TASP699 is a novel PET radiotracer with high affinity and selectivity for the V_{1B}R. The purpose of this study was to characterize the pharmacokinetic and binding profiles of ^{11}C-TASP699 in human and determine its utility in an occupancy study of a novel V_{1B}R antagonist, TS-121.

Methods: Six healthy subjects were scanned twice with ^{11}C-TASP699 to determine the most appropriate kinetic model for analysis of imaging data and test-retest reproducibility of outcome measures. Nine healthy subjects were scanned before and after administration of TS-121 (active component: THY1773) to assess V_{1B}R occupancy. Metabolite-corrected arterial input functions were obtained. Pituitary time-activity curves were analyzed with one- and two-tissue compartment (1TC, 2TC) models and multilinear analysis 1 (MA1) to calculate distribution volumes (V_T). Relative test-retest variability (TRV) and absolute test-retest variability (aTRV) were calculated. Since no brain region could be used as a reference region, percent change in V_T after TS-121 administration was computed to assess its receptor occupancy and correlate with plasma concentration of the drug.

Results: ^{11}C-TASP699 showed high uptake in the pituitary and no uptake in any brain regions. The 2TC model provided better fits than the 1TC model. The MA1 V_T estimates were very similar to the 2TC V_T estimates, so MA1 was the model of choice. TRV of V_T was good (TRV: -2±14%, aTRV: 11%). THY1773 reduced V_T in a dose-dependent fashion, with IC_{50} of 177±52 ng/mL in plasma concentration. There were no adverse events resulting in discontinuation from the study.

Conclusion: ^{11}C-TASP699 was shown to display appropriate kinetics in human with substantial specific binding and good reproducibility of V_T. Therefore, this tracer is suitable for measurement of the V_{1B}R in human pituitary and V_{1B}R occupancy of TS-121, a novel V_{1B}R antagonist.

KEYWORDS

PET, Kinetic modeling, Receptor imaging, Pituitary, Vasopressin V_{1B} receptor

INTRODUCTION

Arginine vasopressin (AVP) is a key regulator of the hypothalamic-pituitary-adrenal (HPA) axis. In response to stress exposure, AVP potentiates the effects of corticotropin-releasing factor on adrenocorticotropin release from pituitary corticotrophs (*1*). Among the three vasopressin receptor subtypes (V_{1A}, V_{1B}, and V_2), the V_{1B} receptor ($V_{1B}R$), which is expressed abundantly in the anterior pituitary (*2*), mediates the pituitary actions of AVP, and regulates HPA axis activity (*3*).

Several clinical studies have reported on the role of AVP in stress-related disorders. For example, AVP plasma levels were elevated in patients with major depressive disorder (MDD) in comparison with healthy controls (*4*), and also in depression with anxiety and slowed psychomotor activity (*5*). Cerebrospinal fluid AVP levels significantly decreased in MDD patients treated with the antidepressant fluoxetine, which is accompanied by a decrease in the depression scores (*6*). In general, hyperactivity of the HPA axis is a common finding in depression (*7,8*) and is thus a target of antidepressant treatment. These findings suggest that $V_{1B}R$ antagonists may be indicated in the treatment of MDD via reducing HPA axis activity (*9,10*).

Development of $V_{1B}R$ imaging agents for PET will permit the in vivo characterization of this receptor subtype in humans, and accurate quantification of target engagement by drug candidates. To date, such development has been hampered by the lack of selective $V_{1B}R$ ligands. A non-peptide $V_{1B}R$ antagonist, ^{11}C-SSR149415, was evaluated in non-human primates and shown to have minimal uptake in the brain and high uptake in the pituitary (*11*). However, human imaging of ^{11}C-SSR149415 has not been reported. More recently, a novel pyridopyrimidin-4-one analog, N-tert-butyl-2-[2-(6-methoxypyridine-2-yl)-6-[3-(morpholin-4-yl)propoxy]-4-oxopyrido[2,3-d]pyrimidin-3(4H)-yl]acetamide (TASP699), was identified as a $V_{1B}R$ antagonist with high affinity and selectivity for $V_{1B}R$ (V_{1B}: 0.16 nM, 87 other off-target molecules including V_{1A}, V_2, and oxytocin receptors: > 1 μM) (*12*). The ^{11}C-labeled ligand, ^{11}C-TASP699, was then developed as a PET radiotracer and shown to have high uptake in the monkey pituitary. Further, the pituitary uptake was dose-dependently inhibited by pretreatment with TASP0390325 (*12*), a selective $V_{1B}R$ antagonist that has been well characterized in pharmacological studies (*13*), thus demonstrating the $V_{1B}R$ binding specificity of ^{11}C-TASP699.

The aim of this first-in-human PET study was to evaluate the tracer ^{11}C-TASP699 for measurement of $V_{1B}R$ availability, to assess the reproducibility of binding parameters. An open-label, single dose study was also done to determine the target occupancy of a novel $V_{1B}R$ antagonist TS-121 (*14*) in the pituitary and to evaluate the relationship between plasma exposure of THY1773 (active component of TS-121) and receptor occupancy.

MATERIALS AND METHODS

Human Subjects

This was a 2-part study: 1) test-retest, and 2) receptor occupancy. A total of 15 healthy male subjects were enrolled (test-retest: n=6, 37–50 y old; body weight, 88±11 kg; occupancy: n=9, 32–52 y old; body weight, 80±10 kg). Individuals were excluded for a diagnosis of a current and/or lifetime psychiatric disorder, current or past serious medical or neurological illness, metal in body which would result in MRI contraindication, or a history of substance abuse or dependence. PET imaging experiments were conducted under a protocol approved by the Yale University School of Medicine Human Investigation Committee and the Yale-New Haven Hospital Radiation Safety Committee and were in accordance with U.S. federal guidelines and regulations for the protection of human research subjects (title 45, part 46, of the *Code of Federal Regulations*). Written informed consent was obtained from all subjects. MR images were acquired on all subjects to verify the absence of brain structural abnormalities. MR imaging was performed on a 3T whole-body scanner (Trio, Siemens Medical Systems). The dimension and pixel size of MR images were 256×256×176 voxels and 0.98×0.98×1.0 mm^3, respectively.

Safety assessments included monitoring of adverse events (AEs) and serious adverse events (SAEs), routine hematology, biochemistry and urinalysis testing, physical/neurological exams, vital signs and electrocardiograms (ECGs), concomitant medications, and extent of exposure (^{11}C-TASP699 exposure in terms of radioactivity [MBq] per kilogram of body weight and total radioactivity, and, for Part 2, extent of exposure to TS-121 in terms of milligrams of drug per kilogram of body weight at admission).

Radiotracer Synthesis

^{11}C-TASP699 (Figure 1) was radiolabeled with ^{11}C-CH_3I as reported previously (*12*). The PET drug was purified by high performance liquid chromatography (HPLC) (Luna C18(2), 10 µm, 10×250 mm, 25% acetonitrile/75% 0.1 M ammonium formate with 0.5% acetic acid, pH 4.2, at 5 mL/min and 254 nm), isolated by solid-phase extraction and formulated in 10 mL saline containing 1 mL ethanol. The detailed radiosynthesis procedure is described in the supplemental material.

PET Imaging Experiments

Six subjects underwent two 2-hour ^{11}C-TASP699 PET scans on one day to measure the reproducibility of the binding parameters in Part 1 of the study. The start of the two scans were separated by 5.3±0.7 hours. In Part 2 of the study, nine subjects completed three 90-minute PET scans (baseline, post-dose 1, post-dose 2) to assess $V_{1B}R$ occupancy in the pituitary following a single oral administration of TS-121. The TS-121 dose was adaptively determined (3 mg, n=1; 10 mg, n=3; 30 mg, n=2; 50 mg, n=3). Post-dose 1 scans were acquired 2.3 hours after the dose of TS-121, and post-dose 2 scans were acquired 1 or 2 days after the dose of TS-121 (3 mg, 2 days; 10 mg, 1 day; 30 mg, 2 days, 50 mg, 1 day [n=2] and 2 days [n=1]). The concentrations of THY1773 in plasma at pre-, mid, and post-scan were determined by liquid chromatography and tandem mass spectrometry at CMIC, Inc. (Hoffman Estates, IL, USA), on behalf of Taisho Pharmaceutical Co., Ltd. (Tokyo, Japan). The measured concentrations were averaged and used as the mean plasma exposure for each post-dose scan.

All PET scans were conducted on the High Resolution Research Tomograph (Siemens Medical Solutions), which acquires 207 slices (1.2 mm slice separation) with a reconstructed image resolution of ~3 mm in full width at half maximum. After a 6-min transmission scan for attenuation correction, PET scans were acquired in list mode following intravenous administration of ^{11}C-TASP699 over 1 min by an automatic pump (Harvard PHD 22/2000, Harvard Apparatus, Holliston, MA, USA). Dynamic scan data were reconstructed in 33 (test-retest) or 27 (occupancy) frames (6×0.5 min, 3×1 min, 2×2 min, 22 or 16×5 min) with corrections for attenuation, normalization, scatter, randoms, and deadtime using the MOLAR algorithm (*15*). Event-by-event motion correction (*16*) was included in the reconstruction

based on measurements with the Polaris Vicra sensor (NDI Systems, Waterloo, Canada) with reflectors mounted on a swim cap worn by the subject.

In four scans, the Vicra motion-tracking signal was unstable or lost due to slip of the cap, so head motion was estimated by registration of the emission images reconstructed without attenuation or scatter corrections, and then dynamic PET images were reconstructed using the estimated motion. For four other scans, small residual motion was visible, so each image frame was aligned to the early average image from 0 to 10 min post-injection.

Input Function Measurement

Arterial input functions were generated for all scans. Discrete blood samples were manually drawn every 10 seconds from 10 to 90 seconds, every 15 seconds from 90 seconds to 3 min, and then at 3.5, 5, 6.5, 8, 12, 15, 20, 25, 30, 45, 60, 75, and 90 min, 105, and 120 min. In addition to samples for the whole blood and plasma radioactivity curves, arterial blood samples were drawn for determination of the unmetabolized fraction of tracer: at 3, 8, 15, 30, 60 and 90 min for test-retest scans and at 5, 15, 30, 60, and 90 min for occupancy scans. Radiometabolite analysis was performed using the column-switching HPLC method (*17*). Briefly, plasma was separated from the whole blood by centrifugation. Up to 5 mL of filtered plasma samples treated with urea (8M) were injected to the automatic column-switching system equipped with a capture column (19×4.6 mm) packed with Phenomenex SPE Strata-X sorbent and a Phenomenex Luna C18(2) analytical column (5 μm, 4.6×250 mm) eluting with 1% acetonitrile in water at a flow rate of 2 mL/min for the first 4 min, then with a mobile phase of 31% acetonitrile and 69% 0.1 M ammonium formate (v/v) at 1.85 mL/min. The unmetabolized parent fraction was determined as the ratio of the sum of radioactivity in fractions containing the parent compound (retention time of ~10.5 min) to the total radioactivity collected, and fitted with inverted gamma function.

For one baseline scan, reliable metabolite data were not available, so the parent fraction curve at the post-dose 2 study was used to calculate a metabolite-corrected input function. For one post-dose

2 scan, arterial blood samples were not available, so the input function from the baseline scan was scaled using the ratio of the injected doses between the 2 scans.

An ultrafiltration-based method was used to measure the unbound portion (free fraction, f_P) of ^{11}C-TASP699 in plasma (*18*).

Quantitative Analysis

Analysis was performed directly on the PET images. A pituitary region of interest (ROI) was determined as the 400 voxels (730 mm^3) with the highest values on the SUV image (test-retest scans: 10–120 min, occupancy scans: 10–90 min), and a pituitary time-activity curve (TAC) was generated. The ROI was chosen to be larger than the pituitary size to reduce viability across frames. The value of regional distribution volume (V_T) was computed using one-tissue and two-tissue compartment (1TC, 2TC) models, and the multilinear analysis 1 (MA1) method. The effect of inclusion of a blood volume term was also assessed. The *F* test was used to compare model fits. Data points were weighted based on noise equivalent counts in each frame. Percentage standard error (%SE) was estimated from the theoretical parameter covariance matrix.

The mean and SD of the test-retest variability (TRV) was calculated as follows:

$$\mathrm{TRV} = 100 \times \frac{V_T^{\mathrm{retest}} - V_T^{\mathrm{test}}}{(V_T^{\mathrm{retest}} + V_T^{\mathrm{test}})/2}$$

Mean TRV is an index of trend in V_T values between test and retest scans, and SD of TRV is an index of the variability of the percentage difference between the two measurements. The absolute value of TRV (aTRV), which combines these two effects into a single value, was also computed.

The time-stability of pituitary V_T values were assessed by comparing V_T from shortened scans from 110 to 50 min, to those from 120-min V_T in the test-retest dataset. Two criteria were used to determine a minimum scan duration (*19*): a) the average of the ratio was between 0.95 and 1.05; b) the inter-individual SD of the ratio was < 0.1.

For the occupancy study, the fractional difference, i.e., apparent receptor occupancy (*aRO*), between baseline and post-dose V_T values was computed using the following formula, which also shows the physiological interpretation of *aRO*.

$$aRO = 1 - \frac{V_T^{\text{post-dose}}}{V_T^{\text{baseline}}} = 1 - \frac{V_{ND}(1+BP_{ND}(1-RO))}{V_{ND}(1+BP_{ND})} = RO\,\frac{BP_{ND}}{1+BP_{ND}} \quad (1)$$

V_{ND} is the nondisplaceable volume of distribution, BP_{ND} is the pituitary binding potential with respect to the nondisplaceable pool, and *RO* is the true receptor occupancy. Since *aRO* is proportional to *RO*, the IC_{50} of THY1773 can be estimated with the following formula using the plasma concentration and *aRO*.

$$aRO = aRO_{\max}\frac{C}{IC_{50}+C} \quad (2)$$

where aRO_{max} is the maximum possible value of *aRO* $[BP_{ND}/(1+BP_{ND})]$ and *C* is THY1773 plasma concentration during each scan.

All modeling was performed with in-house programs using IDL 8.0 (ITT Visual Information Solutions, Boulder, CO, USA).

RESULTS

Radiochemistry

^{11}C-TASP699 was prepared in 24±6% radiochemical yield based on trapped ^{11}C-CH_3I (range: 7.3 to 44.1% for *n*=41, decay corrected to the end of bombardment). At end of synthesis, the radiochemical and chemical purities were 97 ± 2% and 99±7%, respectively, and the molar activity was 1017.1±465.0 GBq/μmol (173.5–1910 GBq/μmol). The average synthesis time was 46±2 min.

Injection Parameters and Plasma Analysis

Table 1 lists the injected radioactivity dose, molar activity at time of injection, injected mass, and plasma free fractions. There were no significant differences between test and retest scans or between baseline and post-dose scans. Administered activity of ^{11}C-TASP699 was 569±169 MBq (range, 301–756 MBq) for the test-retest study and 533±118 MBq (range, 312–707 MBq) for the occupancy study. There were no adverse or clinically detectable pharmacological effects by the administered radiotracer in any subject. No significant changes in vital signs or the results of laboratory studies were observed.

Figure 2 shows mean±SD of parent fractions and metabolite-corrected plasma curves. In Part 1, the mean parent fractions at 30 min were 71±7% for the test scans (*n*=6) and 69±6 % for the retest

scans (n=6), and in Part 2, 70±3% for the baseline scans, 69±3% for post-dose scan 1, and 69±6% for post-dose scan 2. The free fraction (f_P) of ^{11}C-TASP699 in plasma was 48 ± 6% (n=12, test-retest), 50±7% (n=9, baseline), 51 ± 5% (n=9, post-dose scan 1), and 52 ± 6% (n=9, post-dose scan 2). The free fraction displayed no difference between test and retest scans or between baseline and post-dose scans.

Modeling Results

High uptake of ^{11}C-TASP699 was reliably seen in the pituitary with no substantial uptake in brain regions, such as choroid plexus and pineal gland (Figure 3-B). Pituitary regional TACs of ^{11}C-TASP699 (Figure 4) showed peak uptake at 10~30 min post-injection followed by gradual clearance. Typical examples of fits are shown in Figure 4-A. The pituitary TAC was fitted well with the 2TC and MA1 models, and the F-test showed that 2TC fitting was better than the 1TC model ($P < 0.05$ in 11 out of 12 fits). However, the 2TC model provided unstable V_T estimation (relative SE > 10%) and physiologically implausible micro-parameters (relative SE of K_1 and k_2 > 100%). The mean pituitary K_1 from 1TC was 0.10±0.02 mL/cm^3/min. 1TC V_T estimates were somewhat underestimated compared to the reliable 2TC values, but showed a good correlation with 2TC V_T estimates ($V_{T,1TC} = 0.91 \times V_{T,2TC} + 0.11, R^2 = 0.99$). MA1 V_T estimates were similar to those from 2TC with a good correlation ($V_{T,MA1,t^*=10min} = 0.97 \times V_{T,2TC} + 0.21, R^2 = 1.00$). Since the MA1 method provided reliable V_T estimates (relative SE < 10%) similar to those from 2TC, the MA1 V_T values were used in the following analysis.

MA1 V_T values showed large intersubject variability, ranging from 3.6 to 9.7 mL/cm^3 (n = 19; test, retest, and baseline scans), and ~15 mL/cm^3 for one subject, which may have been caused in part by the ROI definition. Note, however, that the TRV and aTRV were reasonably good (TRV: -2 ± 14%, aTRV: 11%, ICC: 0.94) (Figure 5-A), indicating good reliability of the measurements from repeated scans. The V_T estimates for all models did not change with the inclusion of 2 additional parameters: a blood volume term and the time delay between the blood sampling site and pituitary. The percent differences were 3±3% (1TC), 4±3% (2TC), and 0±2% (MA1). Note that many 2TC V_T values were unstable with the addition of delay and blood volume parameters (8 out of 20 fits), and these values

were excluded from this comparison. Pituitary blood volume was estimated to be ~20%. The minimum scan time for stable MA1 V_T estimates was 90 min. Percent difference of V_T with respect to 120-min estimate was -6±13%, -2±16%, 1±14%, 1±9%, 0±6%, and 0±3% for the 60 min, 70 min, 80 min, 90 min, 100 min, and 110 min scan duration.

Occupancy Results

Figure 4-B shows a set of pituitary TACs from the baseline and post-dose scans after a 10 mg dose of TS-121. A moderate blocking effect was observed in the pituitary region. Figure 5-B summarizes the percent reductions in V_T in the pituitary using MA1, while Figure 6 shows a plot of the %change in V_T with THY1773 concentration in the plasma. THY1773 plasma concentration over time is shown in Supplemental Figure 1. Using Eq. 2, the IC_{50} (mean±SE) was estimated at 177±52 ng/mL, with aRO_{max} of 62±7%. Using the estimated aRO_{max} and Eq. 1, the pituitary binding potential (BP_{ND}), representing the equilibrium ratio of specific to non-displaceable binding, was calculated to be 1.6. Using the estimated aRO_{max}, %change in V_T was converted to RO, shown as the y axis on the right of Figure 6.

In fitting PET-measured occupancy values, it is typically assumed that the plasma drug levels are an accurate reflection of the drug levels in the tissue. This assumption may not be met at early times depending on how rapidly the drug enters the tissue (*20*). We thus assessed whether the occupancy values at all times were consistent by using the F-test to compare regression curve fits of Eq. 2. The null hypothesis was that one set of model parameters was appropriate for all post-dose scans. The alternative hypothesis was that a different curve was needed for the post-dose scan 1 data vs. the post-dose scan 2 data, due to potential hysteresis. The null hypothesis was not rejected (P = 0.29). Therefore, hysteresis was not considered in the estimation. However, the ability to detect hysteresis may be limited since the data points for post-dose 1 and post-dose 2 scans were centered on different concentrations of the curve.

Safety

Overall, no safety issues were identified that would prevent further development and testing of both the investigational radiotracer ^{11}C-TASP699 and the investigational drug TS-121.

No SAEs or AEs resulting in discontinuation from the study (pain or burning at arterial line/injection sites was the most common AE, occurring in 3 subjects). No apparent safety trends in clinical laboratory results, vital sign measurements, ECG results, or physical and neurological exams were observed.

DISCUSSION

This first-in-human PET study was conducted to assess the ability of a novel V_{1B}R antagonist PET radiotracer, ^{11}C-TASP699, to image V_{1B}R in the human pituitary. Modeling methods were evaluated based on time-activity curves and metabolite-corrected input functions. The volume of distribution was determined and used to estimate receptor occupancy by the V_{1B}R antagonist, TS-121. A clear relationship between plasma concentration of the drug and receptor occupancy was found.

Modeling analysis assumes that only parent compound enters tissue and binds to the receptor. However, radiolabeled metabolites are likely to access the pituitary, since it has no blood-brain barrier. If the magnitude of the metabolite effect was large, it could bias the results. This does not seem to be the case, since 1) V_T did not show a continuous increase with scan time, as would be expected from tissue uptake of metabolites, and 2) the metabolite fraction in plasma was moderate. In addition, since the fraction of metabolites was similar in the baseline and post-dose scans, even if radiolabeled metabolites were present, and incorrectly increasing estimated V_T values, the IC_{50} estimates would likely not be affected although the maximum occupancy (aRO_{max}) could be biased.

Large intersubject variability was seen in V_T (4 to 10 mL/cm^3), although the test-retest reproducibility was good (aTRV: 11%). We evaluated whether there was a relationship between V_T estimates at baseline scans and subject age, weight, body-mass index, scan starting time, and injected mass, but found no significant effects. The pituitary volume itself might affect V_T, since it varies by age, gender, season, and subject conditions (*21-23*). However, we were not able to accurately define pituitary volumes from MR images since separation of the pituitary from neighboring tissues was challenging in many cases. Thus, we used a standard ROI size. Mean pituitary volume in healthy males is 500 ± 79 mm^3 (*22*), and a larger ROI (730 mm^3) was used to ensure that all uptake was included. To further

consider this factor, the effect of ROI size on V_T values was evaluated. As expected, V_T values increased with smaller ROI sizes, due to reduced partial volume effect. Near-identical test-retest variability was found for ROI sizes above 500 mm^3 (TRV: -3±15% with 550 mm^3 and -2±13% with 910 mm^3). Thus, the large intersubject variability in $V_{1B}R$ could have some biological meanings. There have been several studies using immunohistochemistry, RT-PCR, and in situ hybridization histochemistry to investigate $V_{1B}R$ distribution in rodents. However, to the best of our knowledge, there are no quantitative postmortem studies in humans or non-human primates.

For the two subjects for whom plasma or metabolite data were not available from one scan, the data from another scan were used to generate the input function. We evaluated the effect of using these data from other scans in the subjects where all data were available. Percent differences in V_T were 1 ± 8% (plasma) and 0 ± 4% (metabolites).

Using ^{11}C-TASP699, we evaluated the $V_{1B}R$ occupancy of TS-121, a drug candidate targeted for MDD. Based on animal model experience with THY1773, attenuated hyperactivity of HPA axis and antidepressant-like effects were found with >50% pituitary $V_{1B}R$ occupancy. This study showed that 10–50 mg of TS-121 achieved >50% occupancy at 2 hours after a single oral administration in healthy male subjects (Figure 6). A Phase 2 clinical trial using TS-121 (*14*) in MDD patients showed reductions in the Montgomery-Asberg Depression Rating Scale score for subjects who had a daily oral TS-121 dose of 10 or 50 mg at week 6, though these reductions did not achieve statistical significance. If the plasma concentration was similar in both groups (MDD patients with daily dosing, and our healthy subjects with a single administration), then the dose of 10–50 mg should have been sufficient. However, plasma concentration may differ between patients and healthy subjects, as was seen in a glycine transporter-1 inhibitor study (*24*), where the IC_{50} was similar between healthy controls and schizophrenic patients, but the ID_{50} values were significantly different.

CONCLUSION

The novel $V_{1B}R$ antagonist tracer ^{11}C-TASP699 showed high uptake in the pituitary but did not enter the brain. Its tracer kinetics could be modeled using MA1 to quantify distribution volume. V_T

values were variable between subjects, but showed good test-retest reproducibility. ^{11}C-TASP699 was successfully used in an occupancy study that showed a consistent relationship between THY1773 (active component of TS-121) plasma concentration and V_{1B}R occupancy. Single oral doses of TS-121 (3 mg, 10 mg, 30 mg, and 50 mg) were found to be safe and well-tolerated.

DISCLOSURE

This study was funded by Taisho Pharmaceutical R&D Inc. Izumi Nishino is a full-time employee of Taisho Pharmaceutical Co., Ltd. Satoshi Ozaki and Helene Sabia are a full-time employees of Taisho Pharmaceutical R&D Inc. Ming-Rong Zhang and Tetsuya Suhara hold a patent for ^{11}C-TASP699 (Japan patent JP2015-1206 44A). No other potential conflict of interest relevant to this article was reported.

KEY POINTS

QUESTION: Does ^{11}C-TASP699 show suitable kinetic properties to quantify pituitary V_{1B}R in humans?

PERTINENT FINDINGS: The novel V_{1B}R antagonist tracer ^{11}C-TASP699 showed a good test-retest reproducibility. The tracer showed high uptake in the pituitary but did not enter the brain. The occupancy of TS-121 increased in a dose-dependent fashion (IC_{50} was 177 ng/mL as THY1773).

IMPLICATIONS FOR PATIENT CARE: ^{11}C-TASP699 provides the excellent measurements of V_{1B}R binding in the human pituitary.

References

1. Aguilera G, Rabadan-Diehl C. Vasopressinergic regulation of the hypothalamic-pituitary-adrenal axis: implications for stress adaptation. *Regul Pept.* 2000;96:23-29.
2. Serradeil-Le Gal C, Raufaste D, Derick S, et al. Biological characterization of rodent and human vasopressin V1b receptors using SSR-149415, a nonpeptide V1b receptor ligand. *Am J Physiol Regul Integr Comp Physiol.* 2007;293:R938-949.
3. Tanoue A, Ito S, Honda K, et al. The vasopressin V1b receptor critically regulates hypothalamic-pituitary-adrenal axis activity under both stress and resting conditions. *J Clin Invest.* 2004;113:302-309.
4. van Londen L, Goekoop JG, van Kempen GM, et al. Plasma levels of arginine vasopressin elevated in patients with major depression. *Neuropsychopharmacology.* 1997;17:284-292.
5. de Winter RF, van Hemert AM, DeRijk RH, et al. Anxious-retarded depression: relation with plasma vasopressin and cortisol. *Neuropsychopharmacology.* 2003;28:140-147.
6. De Bellis MD, Gold PW, Geracioti TD, Jr., Listwak SJ, Kling MA. Association of fluoxetine treatment with reductions in CSF concentrations of corticotropin-releasing hormone and arginine vasopressin in patients with major depression. *Am J Psychiatry.* 1993;150:656-657.
7. Scott LV, Dinan TG. Vasopressin and the regulation of hypothalamic-pituitary-adrenal axis function: implications for the pathophysiology of depression. *Life Sci.* 1998;62:1985-1998.
8. Inder WJ, Donald RA, Prickett TC, et al. Arginine vasopressin is associated with hypercortisolemia and suicide attempts in depression. *Biol Psychiatry.* 1997;42:744-747.
9. Griebel G, Stemmelin J, Gal CS, Soubrie P. Non-peptide vasopressin V1b receptor antagonists as potential drugs for the treatment of stress-related disorders. *Curr Pharm Des.* 2005;11:1549-1559.
10. Roper J, O'Carroll AM, Young W, 3rd, Lolait S. The vasopressin Avpr1b receptor: molecular and pharmacological studies. *Stress.* 2011;14:98-115.
11. Schonberger M, Leggett C, Kim SW, Hooker JM. Synthesis of [11C]SSR149415 and preliminary imaging studies using positron emission tomography. *Bioorg Med Chem Lett.* 2010;20:3103-3106.
12. Koga K, Nagai Y, Hanyu M, et al. High-Contrast PET Imaging of Vasopressin V1B Receptors with a Novel Radioligand, (11)C-TASP699. *J Nucl Med.* 2017;58:1652-1658.
13. Iijima M, Yoshimizu T, Shimazaki T, et al. Antidepressant and anxiolytic profiles of newly synthesized arginine vasopressin V1B receptor antagonists: TASP0233278 and TASP0390325. *Br J Pharmacol.* 2014;171:3511-3525.
14. Kamiya M, Sabia HD, Marella J, et al. Efficacy and safety of TS-121, a novel vasopressin V1B receptor antagonist, as adjunctive treatment for patients with major depressive disorder: A randomized, double-blind, placebo-controlled study. *J Psychiatr Res.* 2020;128:43-51.

15. Carson RE, Barker WC, Liow JS, Johnson CA. Design of a motion-compensation OSEM list-mode algorithm for resolution-recovery reconstruction for the HRRT. *IEEE 2003 Nuclear Science Symposium Conference Record.* 2003;5:3281-3285.
16. Jin X, Chan C, Mulnix T, et al. List-mode reconstruction for the Biograph mCT with physics modeling and event-by-event motion correction. *Phys Med Biol.* 2013;58:5567-5591.
17. Hilton J, Yokoi F, Dannals RF, Ravert HT, Szabo Z, Wong DF. Column-switching HPLC for the analysis of plasma in PET imaging studies. *Nucl Med Biol.* 2000;27:627-630.
18. Li S, Cai Z, Zheng MQ, et al. Novel (18)F-labeled kappa-opioid receptor antagonist as PET radiotracer: synthesis and in vivo evaluation of (18)F-LY2459989 in nonhuman primates. *J Nucl Med.* 2018;59:140-146.
19. Frankle WG, Huang Y, Hwang DR, et al. Comparative evaluation of serotonin transporter radioligands ^{11}C-DASB and ^{11}C-McN 5652 in healthy humans. *J Nucl Med.* 2004;45:682-694.
20. Naganawa M, Gallezot JD, Rossano S, Carson RE. Quantitative PET imaging in drug development: estimation of target occupancy. *Bull Math Biol.* 2019;81:3508-3541.
21. Lurie SN, Doraiswamy PM, Husain MM, et al. In vivo assessment of pituitary gland volume with magnetic resonance imaging: the effect of age. *J Clin Endocrinol Metab.* 1990;71:505-508.
22. Schwartz PJ, Loe JA, Bash CN, et al. Seasonality and pituitary volume. *Psychiatry Res.* 1997;74:151-157.
23. Buschlen J, Berger GE, Borgwardt SJ, et al. Pituitary volume increase during emerging psychosis. *Schizophr Res.* 2011;125:41-48.
24. D'Souza DC, Carson RE, Driesen N, et al. Dose-related target occupancy and effects on circuitry, behavior, and neuroplasticity of the glycine transporter-1 inhibitor PF-03463275 in healthy and schizophrenia subjects. *Biol Psychiatry.* 2018;84:413-421.

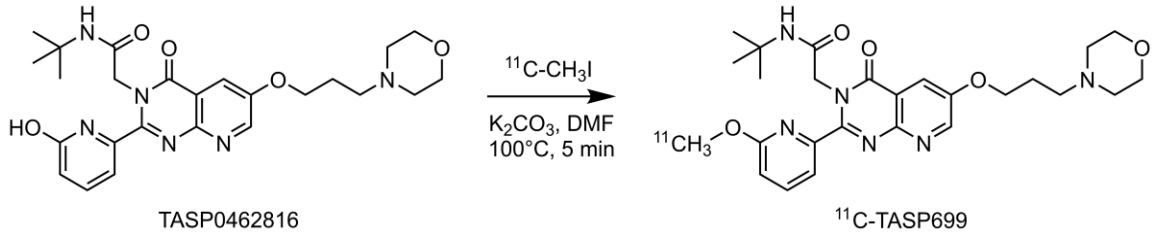

Figure 1: Synthesis of ^{11}C-TASP699.

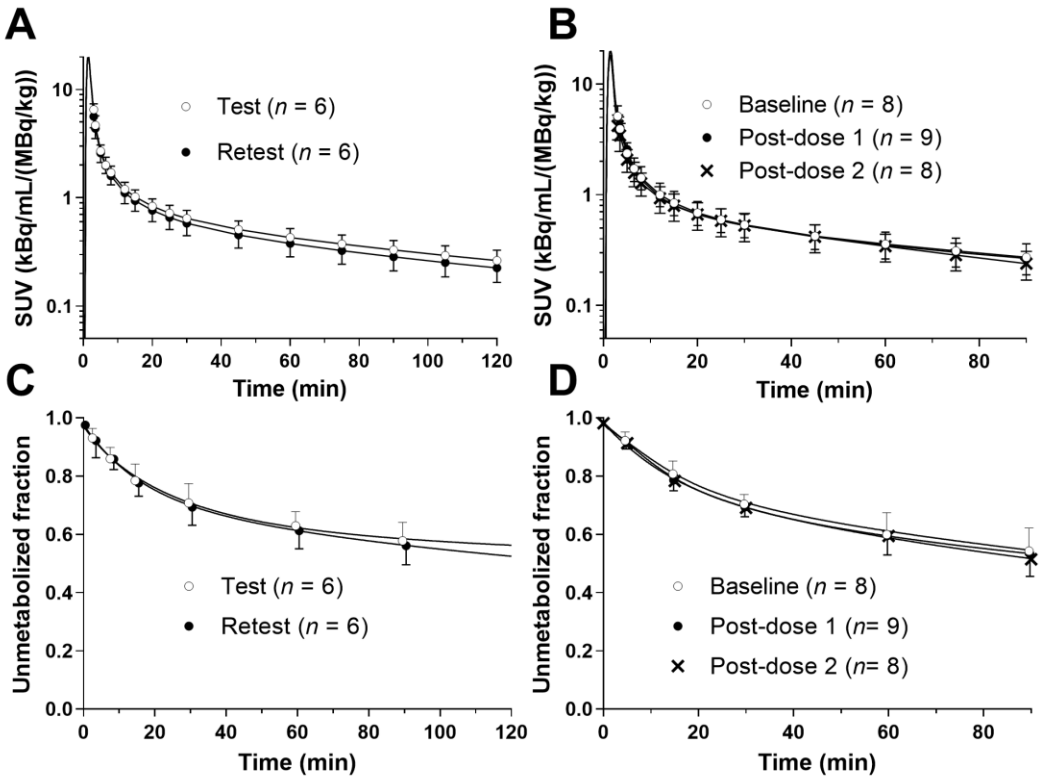

Figure 2: Mean±SD of total plasma activity and parent fraction in the plasma in the test and retest scans (A, C) and in the baseline, post-dose 1, and post-dose 2 scans (B, D).

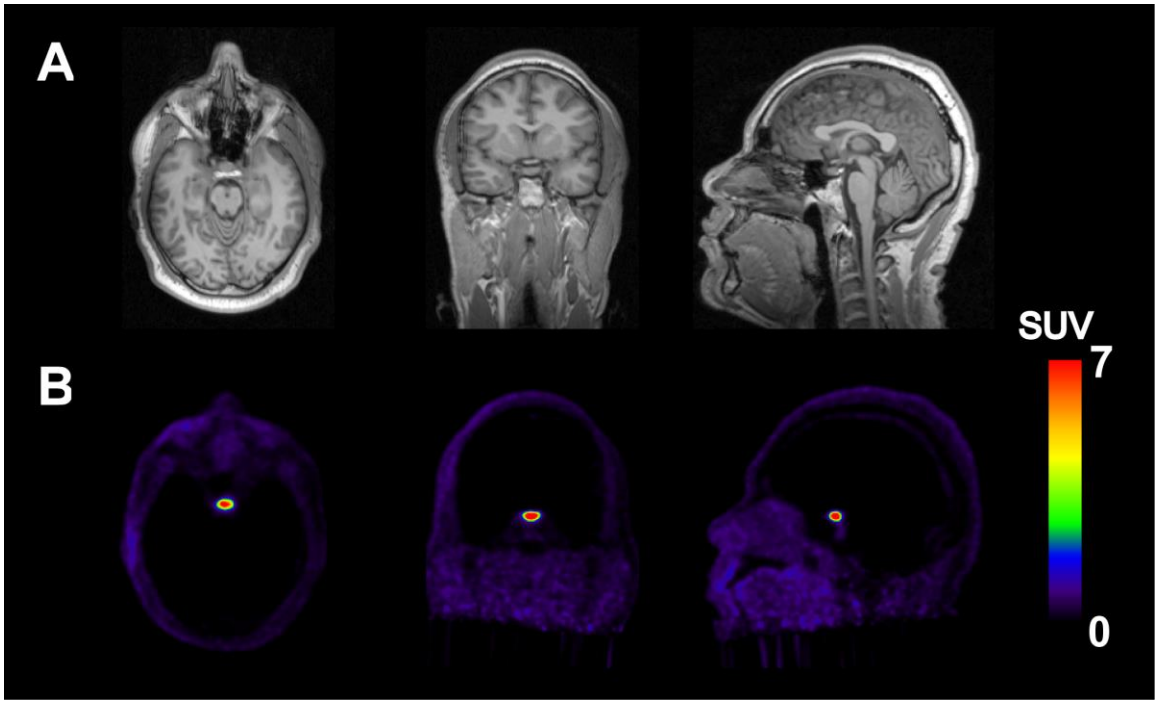

Figure 3: Typical MR (A) and co-registered PET images summed from 30 to 120 min after injection of ^{11}C-TASP699. The coregistration (rigid transform) was applied using extracranial uptake (blue or purple area).

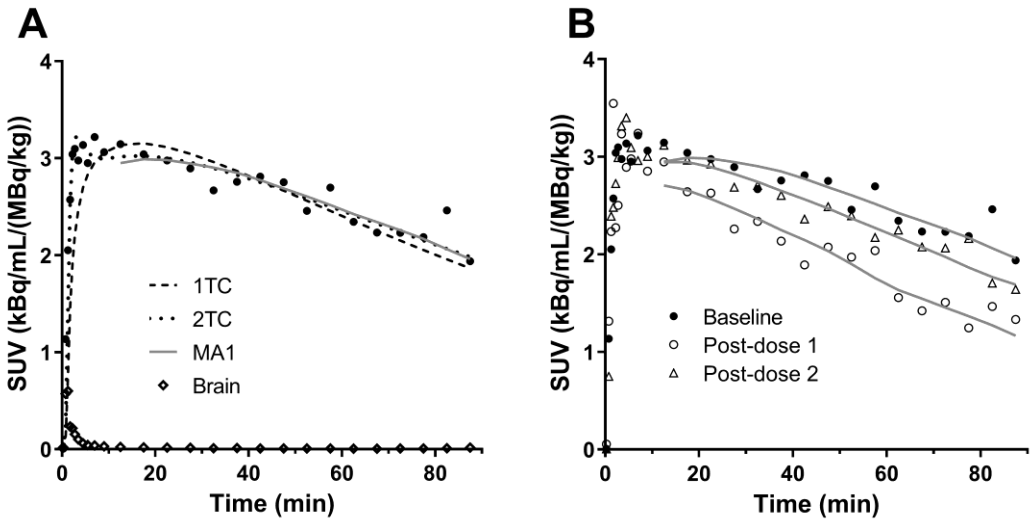

Figure 4: (A) Representative pituitary time-activity curve in a baseline scan with the 1TC (dashed), 2TC (dotted), and MA1 (t^*=10 min, solid) fits with brain time-activity curve. (B) Pituitary time-activity curves in baseline, post-dose 1, and post-dose 2 conditions with the MA1 fits.

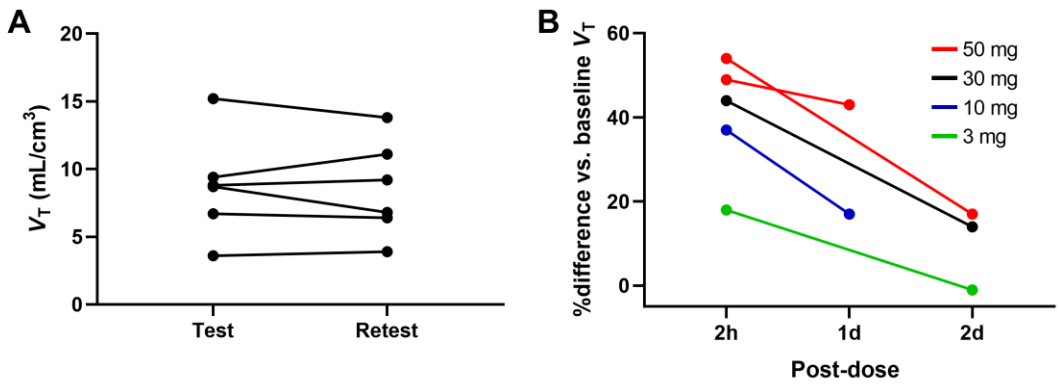

Figure 5: (A) Pituitary V_T values in the test and retest conditions. Each symbol corresponds to a subject. (B) Mean percent difference of V_T in comparison with the baseline V_T values (*aRO*) at 2 hours, 1 day and 2 days after administration of TS-121.

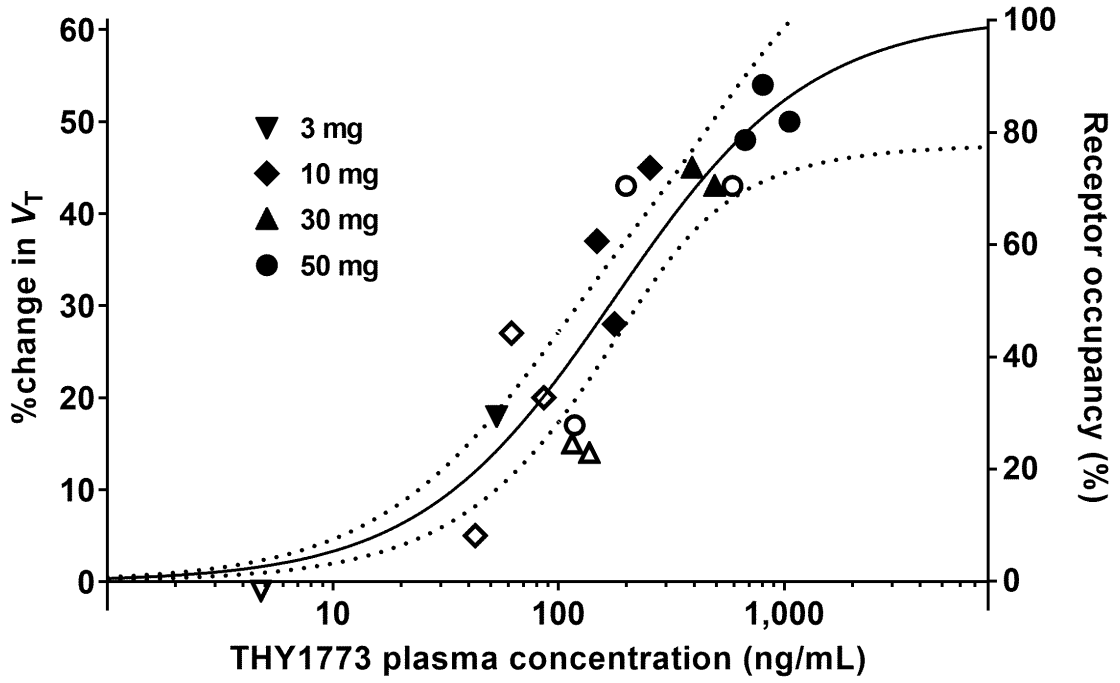

Figure 6: Relationship between THY1773 (active component of TS-121) plasma concentrations and %change in V_T (left *y*-axis) and receptor occupancy (right *y*-axis). Estimated IC_{50} and aRO_{max} are 177±52 ng/mL and 62±7%, respectively. Closed symbols and open symbols denote post-dose 1 and post-dose 2, respectively.

Table 1: PET Scan Parameters

	Test-retest (*n*=6)		Occupancy (*n*=9)		
	Test	Retest	Baseline	Post-dose 1	Post-dose 2
Injected dose (MBq)	618±134	519±196	528±126	540±132	532±109
Injected mass (μg)	0.90±0.57	0.75±0.59	1.16±1.13	1.19±1.19	0.93±0.48
Plasma free fraction	47±5%	50±7%	50±7%	51±5%	52±6%

Graphical Abstract

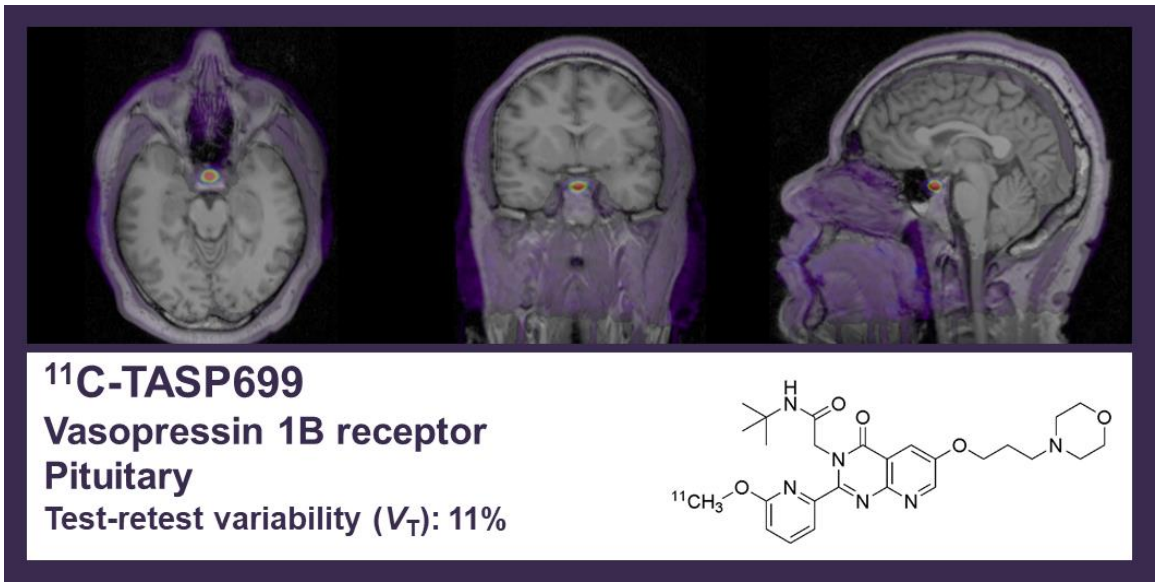

Radiosynthesis of ^{11}C-TASP699

^{11}C-TASP699 was radiolabeled with ^{11}C-CH_3I as reported previously, with minor modifications to the semi-preparative HPLC method and the final product work-up and formulation procedures. Briefly, ^{11}C-CH_3I was swept with helium through a solution of anhydrous DMF (300 µL) at 23°C containing the precursor (0.9-1.5 mg) and K_2CO_3 (8-12 mg), and the resulting solution was heated at 100°C for 5 min. After cooling, the crude mixture was diluted with a mixture of 1.2 mL mobile phase (*vide infra*) and 0.3 mL 0.3 N HCl, then purified by semi-preparative HPLC (Luna C18(2), 10 µm, 10 × 250 mm, 25% acetonitrile/75% 0.1 M ammonium formate with 0.5% acetic acid, pH 4.2, at 5 mL/min and 254 nm). The product fraction (t_R ~10.5-11.5 min) was diluted with 50 mL de-ionized water and passed through a C18 SPE cartridge. The cartridge was washed with 10 mL de-ionized water. The radiolabeled product was eluted from the cartridge with 1 mL ethanol followed by 10 mL saline. The combined ethanol saline mixture was passed through a 0.22 micron sterile membrane filter for terminal sterilization and collected in a sterile pyrogen free collection vial to afford a formulated I.V. solution of ^{11}C-TASP699 ready for dispensing and administration. Chemical purity, radiochemical purity, and molar activity were determined by HPLC (Luna C18(2), 5 µm, 250 × 4.6 mm, 28% acetonitrile/72% 0.1 M ammonium formate, at 2 mL/min and 300 nm).

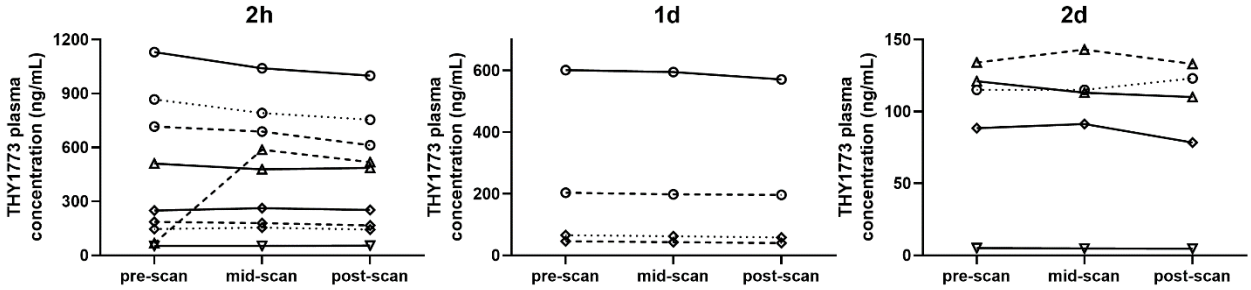

Supplemental figure 1: THY1773 plasma concentration at pre-, mid-, and post-PET scan (3 mg: downward triangles;10 mg, diamonds; 30 mg: triangles, 50 mg: circles).